The influence of the cylindrical shape of the nucleosomes and H1 defects on properties of chromatin

Philipp M. Diesinger[1]
Department of Physics
Institut für theoretische Physik
Heidelberg University
Germany

Dieter W. Heermann
Department of Physics
Institut für theoretische Physik
and
Interdisziplinäres Zentrum
für Wissenschaftliches Rechnen
Heidelberg University, Germany

[1]Corresponding author. Address: Institut für theoretische Physik, Philosophenweg 19, D-69120 Heidelberg, Germany, Tel.: (+49)6221-54-9449, Fax: (+49)-6221-549-331, email: diesinger@tphys.uni-heidelberg.de

Abstract

We present a model improving the two-angle model for interphase chromatin (E2A model). This model takes into account the cylindrical shape of the histone octamers, the H1 histones in front of the nucleosomes and the vertical distance d between the in and outgoing DNA strands. Factoring these chromatin features in, one gets essential changes in the chromatin phase diagram: Not only the shape of the excluded-volume borderline changes but also the vertical distance d has a dramatic influence on the forbidden area. Furthermore, we examined the influence of H1 defects on the properties of the chromatin fiber. Thus we present two possible strategies for chromatin compaction: The use of very dense states in the phase diagram in the gaps in the excluded volume borderline or missing H1 histones which can lead to very compact fibers. The chromatin fiber might use both of these mechanisms to compact itself at least locally. Line densities computed within the model coincident with the experimental values.

Keywords: chromatin, phase diagram, cylindrical nucleosomes, histone H1, excluded volume interaction, Monte Carlo method

Introduction

The nucleosome is the basic repeat unit of chromatin (1) in all eucaryotic organisms. It consists of a cylindrical-shaped histone octamer and a stretch of DNA which is wrapped around the histone complex approximately 1.65 times. The histone octamer consists of four pairs of core histones (H2A, H2B, H3 and H4) and is known up to atomistic resolution (2, 3). The nucleosomes are connected by blank DNA strands and together with these linkers they form the so-called 30nm fiber. The histone H1 (and the variant histone H5 with similar structure and functions) is involved in the packing of the beads on a string structure into the 30nm chromatin structure. To do so it sits in front of the nucleosome keeping in place the DNA which is wrapped around the histone octamer and thus stabilizes the chromatin fiber. The nucleosome provides the lowest level of compaction and, furthermore, it is important in the regulation of transcription. Several enzymes can change the position of the nucleosome (4) to make the genetic information which is held within the nucleosome core particle accessible.

The compaction of the DNA plays a very important role in modern biophysics since it has a total length of some meters but has to fit into a nucleus of some microns. The degree of compaction depends on the salt concentration (5) and on the presence of linker histones (6). The presence of the linker histones leads to the formation of stem-like structures which are formed by the incoming and outcoming DNA string in front of the nucleosome. At low salt concentration a 10nm structure is formed which has the shape of beads on a string (5) whereas at high salt concentrations the chromatin fiber is much more compact and has a diameter of 30nm (7).

The chromatin structure is still not completely understood (1, 8, 9, 10). There are competing models for its structure: zigzag ribbon models (6, 11, 12, 13, 14), helical solenoid models (5, 15, 16), superbeads or simply having no regular structure (17). A crystal structure of a tetranucleosome has been revealed (11) and used to construct a model for the 30nm fiber which resembles a zigzag ribbon that twists or supercoils. The chromatin fiber has been investigated by electron cryo-microscopy (6, 18), atomic force microscopy (19, 20) neutron scattering and scanning transmission electron microscopy (21). Beyond the 30nm level chromatin is poorly understood.

The two-angle model was introduced by Woodcock et al. (12) to describe the geometry of the 30nm chromatin fiber. It has been shown that the

excluded volume of the histone complex plays a very important role for the stiffness of the chromatin fiber (22) and for the topological constraints during condensation/decondensation processes (23). In (24) a rough approximation of the forbidden surface in the chromatin phase diagram was given. In a previous work of ours (25) we answered questions concerning the fine structure of the excluded volume borderline which separates the allowed and forbidden states in the phase diagram with the basic assumption of spherical nucleosomes and no vertical shift between in and outgoing strand. Here we present a Ramachandran-like diagram for chromatin fibers with cylindrical nucleosomes for a new extended model and furthermore discuss the influence of a vertical shift between the linkers due to H1 histones and the volume exclusion of the DNA.

We first present the basic notations for the formulation of the Extended Two-Angle model (E2A). Then we give an algorithm for the generation of chains within the model and present the resulting phase diagram and end-to-end distance as well as radius of gyration results.

Theory

Extended two-angle model

We extend the two-angle model by introducing a parameter for the vertical distance between the DNA strands in front of the nucleosome. Furthermore, we take the cylindrical excluded volume of the nucleosomes into account as well as the H1 histones which fix the DNA linkers in front of the nucleosome. The H1 histones themselves are taken to be random variables to allow for possible missing H1 histones.

Basic notations

We start out and fix some basic notations to use for the formulation of the model. The nucleosomes will be characterized by the centers $N_i \in \mathbb{R}^3$ and the orientations $\hat{p}_i \in \mathbb{R}^3$ of the nucleosomes, with $i = 0, ..., N$ and $\|\hat{p}_i\| = 1$. N is the length of the fiber. The linkers between the centers of two nucleosomes will be denoted by $b_i := N_i - N_{i-1}$ with $i = 1, ..., N$. The length $\|b_i\|$ of the linkers will be a further input parameter of the model (opposite of the *direction* $b_i \in \mathbb{R}^3$ of the linkers). Furthermore, the entry-exit-angle $\alpha_i \in [0, \pi]$ between two consecutive linkers is defined by $\alpha_i := \sphericalangle(-b_i, b_{i+1})$ with $i = 1, ..., N-1$ and the rotational angle $\beta_i \in [0, \pi]$ between two consecutive orientations is given by $\beta_i := \sphericalangle(p_{i-1}, p_i)$ with $i = 1, ..., N$.

Moreover, h_i represents the distance along the orientational axis $\hat{p}_{i-1}$ from N_{i-1} to N_i due to the spatial discrepancy between in and outgoing DNA strand. h_i can be expressed by the vertical distances d_i which the DNA covers by wrapping up itself around the histone complexes: $h_i = \frac{1}{2}(d_{i-1}+d_i)$ with $i = 1, ..., N$.

Thus a single chromatin strand within the two-angle-model is characterized by the following set of variables

$$(\{\alpha_i\}_{i\in\{1,..,N-1\}}, \{\beta_i\}_{i\in\{1,..,N\}}, \{h_i\}_{i\in\{1,..,N\}}, \{\|b_i\|\}_{i\in\{1,..,N\}}).$$

The general rotational matrix $\mathcal{R}$ around an axis $\hat{a} = (a_1, a_2, a_3)^t$ (with $\|\hat{a}\| = 1$) by an angle γ with respect to the right-hand rule will be used in the following. It is given by:

$$\mathcal{R}^{\gamma}_{\hat{a}} = \begin{pmatrix} \cos\gamma + a_1^2(1-\cos\gamma) & a_1a_2(1-\cos\gamma) - a_3\sin\gamma & a_1a_3(1-\cos\gamma) + a_2\sin\gamma \\ a_2a_1(1-\cos\gamma) + a_3\sin\gamma & \cos\gamma + v_2^2(1-\cos\gamma) & a_2a_3(1-\cos\gamma) - a_1\sin\gamma \\ a_3a_1(1-\cos\gamma) - a_2\sin\gamma & a_3a_2(1-\cos\gamma) + a_1\sin\gamma & \cos\gamma + a_3^2(1-\cos\gamma) \end{pmatrix}.$$

Definition of the two-angle model

A chromatin fiber within the framework of the extended two-angle model has to fulfil the following conditions for all $i \in \{1, ..., N\}$:

$$\begin{aligned} &i) \quad \sphericalangle(-b_i, b_{i+1}) = \alpha_i \Leftrightarrow \cos(\alpha_i) = \frac{\langle -b_i, b_{i+1}\rangle}{\|b_i\|\|b_{i+1}\|} \\ &ii) \quad \sphericalangle(\hat{p}_{i-1}, \hat{p}_i) = \beta_i \Leftrightarrow \cos(\beta_i) = \langle \hat{p}_{i-1}, \hat{p}_i\rangle \\ &iii) \quad \|N_i - N_{i-1}\| = \|b_i\| \\ &iv) \quad \langle \hat{p}_{i-1}, b_i\rangle \hat{p}_{i-1} = h_i = \frac{1}{2}(d_{i-1} + d_i). \end{aligned}$$

These are illustrated in Fig 1.

The first condition adjusts the entry-exit angle of nucleosome i to the given parameter α_i. The second condition does the same for the rotational angle due to the DNA twist from nucleosome $i-1$ to nucleosome i. The third condition fixes the distance of the two consecutive nucleosomes $i-1$ and i and the last condition adjusts the vertical distance along the local chromatin axis between the nucleosomes $i-1$ and i.

Construction of the fiber

The construction of the fiber can be done using an iterative process. A further part of the model is the presence of a H1 histone which is assumed to be present with probability p.

The first nucleosome center and its orientation are arbitrary. We chose:

$$N_0 = \begin{pmatrix} 0 \\ 0 \\ 0 \end{pmatrix}, \quad \hat{p}_0 = \begin{pmatrix} 0 \\ 0 \\ 1 \end{pmatrix}.$$

The following vectors fulfil the conditions of the two angle model for the second nucleosome location and its orientation:

$$N_1 = N_0 + \sqrt{\|b_1\|^2 - h_1^2} \begin{pmatrix} -1 \\ 0 \\ 0 \end{pmatrix} + h_1 \hat{p}_0 = \begin{pmatrix} -\sqrt{\|b_1\|^2 - h_1^2} \\ 0 \\ h_1 \end{pmatrix}$$

and

$$\hat{p}_1 = \mathcal{R}_{\hat{a}}^{\beta_1} \hat{p}_{i-1} \quad \text{with} \quad \hat{a} = (1,0,0)^t.$$

Now we can calculate N_{i+1} and $\hat{p}_{i+1}$ in dependence of N_i, N_{i-1}, $\hat{p}_i$ and $\hat{p}_{i-1}$. With

$$v_i := -b_i + \langle \hat{p}_i, -b_i \rangle \hat{p}_i$$

and

$$v_i' := \mathcal{R}_{\hat{p}_i}^{\alpha_0} \sqrt{b_{i+1}^2 - d_{i+1}^2} \left(\frac{v_i}{\|v_i\|} \right) + h_{i+1} \hat{p}_i \tag{1}$$

one gets the location of nucleosome $i+1$ by

$$N_{i+1} = N_i + v_i'.$$

α_0 is the angle between the projections of b_{i+1} and $-b_{i-1}$ onto an arbitrary plane orthogonal to $\hat{p}_i$. We need to calculate the dependence of this projected entry-exit-angle α_0 on the actual entry-exit-angle α.

Note that α_0 was used as entry-exit-angle in some other publications (13, 24) but in this work it denotes only the projection of the real entry-exit-angle α.

Using the law of cosine one gets

$$l^2 = b_i^2 + b_{i+1}^2 - 2 b_i b_{i+1} \cos(\alpha). \tag{2}$$

Now we will use an affine transformation T to a new coordinate system $(x,y,z) \xrightarrow{T} (x',y',z')$ in order to get a second relation for l. We shift the origin to N_i and rotate our old coordinate system so that $\hat{p}_i$ corresponds to the new z-axis. Furthermore, the new x-axis has to coincide with the projection of $-b_i$ onto any plane orthogonal to $\hat{p}_i$.
Obviously,

$$l^2 = \|b_i + v_i'\|^2 = \|b_i' + v_i''\|^2$$

with

$$b_i \xrightarrow{T} b_i' = \begin{pmatrix} \sqrt{b_i^2 - \langle \hat{p}_i, -b_i \rangle^2} \\ 0 \\ \langle \hat{p}_i, -b_i \rangle \end{pmatrix}$$

and

$$v_i' \xrightarrow{T} v_i'' = \begin{pmatrix} \cos(\alpha_0)\sqrt{b_{i+1}^2 - h_{i+1}^2} \\ \sqrt{b_{i+1}^2 - h_{i+1}^2 - \left(\cos(\alpha_0)\sqrt{b_{i+1}^2 - h_{i+1}^2}\right)^2} \\ h_{i+1} \end{pmatrix}.$$

This leads to

$$l^2 = b_{i+1}^2 + b_i^2 - 2h_{i+1}\langle \hat{p}_i, -b_i \rangle - 2\cos(\alpha_0)\sqrt{b_i^2 - \langle \hat{p}_i, -b_i \rangle^2}\sqrt{b_{i+1}^2 - h_{i+1}^2}. \quad (3)$$

By comparing Eq.2 and Eq.3 one gets eventually

$$\cos(\alpha_0) = \frac{b_i b_{i+1}\cos(\alpha) - h_{i+1}\langle \hat{p}_i, -b_i \rangle}{\sqrt{b_{i+1}^2 - h_{i+1}^2}\sqrt{b_i^2 - \langle \hat{p}_i, -b_i \rangle^2}}$$

with the boundary condition

$$\alpha_0 > \alpha_{min} = \operatorname{acos}\left(\frac{(h_{i+1} + \|\langle \hat{p}_i, b_i \rangle\|)^2 - b_{i+1}^2 - b_i^2}{-2b_i b_{i+1}}\right) \quad (4)$$

due to non-vanishing d_i and d_{i+1}. The calculation of N_{i+1} is complete, since we now know the dependence of α_0 on α and therefore one can use Eq.1 to determine N_{i+1}. But one still has to calculate the orientation p_{i+1} of nucleosome N_{i+1}. Due to the fixation of the in and outgoing DNA strand by the H1 histones this orientation can be calculated by a rotation around the following normalized axis $\hat{a}$:

$$\hat{a} := \frac{-b_{i+1} - \langle p_i, -b_{i+1} \rangle \hat{p}_i}{\|\hat{a}\|}.$$

$\hat{p}_{i+1}$ then follows by a rotation of $\hat{p}_i$ around this axis:

$$\hat{p}_{i+1} = \mathcal{R}_{\hat{a}}^{\beta_{i+1}} \hat{p}_i.$$

Methods

Chromatin phase diagram

First we determine the influence of the cylindrical excluded volume of the nucleosomes and a non-vanishing vertical distance between in and outgoing DNA strand on the phase diagram of chromatin. Both of these parameters have been neglected so far (24, 25). To do so we made simulations (26) of regular chromatin fibers and checked whether they fulfil the excluded volume conditions or not. We were able to plot our results in a Ramachandran-like diagram (cf. Fig. 3) and thus find out which states of the whole phase diagram are forbidden by excluded volume interactions and which are not. The fibers we simulated for this part were *regular*, i.e. all linker lengths, entry-exit-angles, rotational angles and h_i were fixed for a certain strand.

The cylinders had a height of $16.8\langle\mathrm{bp}\rangle$, and a diameter of $33.0\langle\mathrm{bp}\rangle$ according to (27). They were orientated by using the vectors p_i above. Moreover, we assumed a DNA diameter of $6.6\langle\mathrm{bp}\rangle$, a twist length of $10.2\langle\mathrm{bp}\rangle$, a mean linker length of $63\langle\mathrm{bp}\rangle$ and that 1.65 turns of DNA are wrapped around the histone octameres.

Fibers with H1 defects

Furthermore, we made Monte Carlo simulations of chromatin fibers with H1 defects, i.e. some of he H1 histones were missing. We used the two-angle-model with some fixed parameters (see above), which reflect the probable mean values within the cell. The only interaction potential is the hard core excluded volume. In this mean field-like approach we neglect (28) thermal fluctuations and thus assume to be above the Θ-point to concentrate on the interaction between H1 defects and volume exclusion.

For a certain nucleosome N_i the defect probability p gives the chance of a missing H1 histone. If the histone is missing the in and outgoing DNA strand are no longer fixed in front of the nucleosome but instead are arbitrary with respect to the excluded volume interactions of the chromatin strand (cf. Fig. 2). Thus we get results for the mean end-to-end distance and the mean radius of gyration of fibers with various defect probabilities: $p = 0.00$, $p = 0.01$, $p = 0.05$, $p = 0.10$ and $p = 0.30$. For these simulations we fixed the entry-exit-angles α_i to 40 degrees, the rotational angles β_i to 36 degrees and $h_i = 7\langle\mathrm{bp}\rangle$.

Results

Phase diagram

The colored lines in Fig. 3 represent the phase transition between allowed and forbidden states. All states below the corresponding line are forbidden, those above it are allowed. The states near the excluded volume borderline are the most interesting of the phase diagram since they are the most compact ones (cf. Fig. 4). Therefore, the gaps in the borderline might be used by the fiber to become (at least locally) very dense.

There is another borderline at the left side of the diagram which prevents α from getting smaller than some minimal value $\alpha_{min}(h)$ which depends on h. This arrow-like structure can be seen best in Fig. 6. It shifts towards larger $\alpha_{min}(h)$ with increasing d. The gap in this line is a further consequence of the *cylindrical* excluded volume and can not be seen in the phase diagram for spherical nucleosomes (25).

As a consequence of the cylindrical instead of spherical excluded volume of the nucleosomes the shape of the peaks in the phase diagram is changed: Their top shows a wedge-like shape due to the edges of the cylinders. With increasing entry-exit-angle α there is more space between the nucleosomes which leads to a larger variety of allowed rotational angles β and thus to the missing tip at the top of the peaks. This effect gets weaker with increasing d: The edges which cut the peaks become more parallel to the α-axis.

With increasing vertical distance between in and outgoing DNA strand there is also more space between consecutive nucleosomes which leads to a decrease of the borderline. More and more states become accessible and with $h = 5.5\langle\text{bp}\rangle$ the borderline almost vanishes. The natural mean value of h is approximately $h = 2.8nm = 8.4\langle\text{bp}\rangle$ due to 1.65 turns of DNA with a diameter of $2.2nm$. Lower h values might occur where the DNA has less turns around the histone complex.

We furthermore examined the line density (cf. Fig. 5) and the radius of gyration (cf. Fig. 6) of regular chromatin fibers (length 500 nucleosomes) along the phase diagram. The most compact states can be found near the excluded volume borderline. The line densities we found in our simulations coincide with experimental values (29). Increasing d decreases the line density and increases the radius of gyration.

H1 defects

We also investigated the influence of missing H1 histones on the mean squared end-to-end distance (Fig. 8) and the mean squared radius of gy-

ration (Fig. 9) of chromatin fibers. The parameter p gives the defect probability in this section. One can clearly see that even very small defect rates of some percent have a huge effect on the compaction of chromatin: Both mean squared radius of gyration and the mean end-to-end distance decrease rapidly if one allows only a few H1 defects. Without H1 defects ($p = 0$) we get an ideal chromatin fiber within the restriction of the extended two-angle model. This ideal fiber reflects the properties of the 30nm strand only on small length scales. Therefore, the increase of the compaction due to defects will probably be not as strong as implicated by our results. Nevertheless missing H1 histones might contribute to chromatin compaction and DNA accessibility for transcription purposes at the same time since one can see from Fig. 7 that although the fiber gets compacter some very open parts appear. One can also see here the increasing disorder with increasing p.

Discussion

The compaction of chromatin is still an open question. A polymer of a total length of two meters has to fit into a tiny cell nucleus of some microns. We showed two possible strategies for the fiber to deal with this task. The fiber might use gaps in the phase diagram, i.e. very dense states to compact parts of itself. Furthermore, we showed that missing H1 histones might supply a further contribution to the compaction of the fiber. These H1 defects might play a very crucial role in the task of chromatin compaction and at the same time serve the transcription of the DNA by opening locally the chromatin fiber.
Moreover, we developed the ordinary two-angle model further to our E2A model, which is much more detailed and thus appropriate to model chromatin at the 30nm level.

Acknowledgements

We thank Giacomo Cavalli, Jörg Langowski and Roel van Driel for fruitful discussions.

References

[1] van Holde, K. E. 1989. Chromatin. Springer-Verlag, New York.

[2] Davey, C.A., Sargent, D.F., Luger, K., Maeder, A.W., Richmond, T.J.

2002. Solvent mediated interactions in the structure of the nucleosome core particle at 1.9 resolution. J. Mol. Biol. Jun 21; 319 (5): 1097-1113.

[3] Luger, K., Mader, A.W., Richmond, R.K., Sargent, D.F., Richmond, T.J. 1997 Crystal structure of the nucleosome core particle at 2.8 angstrom resolution, Nature 389, 251-60.

[4] Lia, G., Praly, E., Ferreira, H., Stockdale, C., Tse-Dinh, Y.C., Dunlap, D., Croquette, V., Bensimon, D., Owen-Hughes, T. 2006 Direct Observation of DNA Distortion by the RSC Complex. Molecular Cell Feb 3; 21 (3): 417-425

[5] Thoma, F., Koller, Th. and Klug, A. 1979. Involvement of histone H1 in the organization of the nucleosome and of the salt-dependent superstructures of chromatin. J. Cell. Biol. 83:403-427.

[6] Bednar, J., Horowitz, R.A., Grigoryev, S.A., Carruthers, L.M., Hansen, J.C., Koster, A.J. and Woodcock, C.L. 1998. Nucleosomes, linker DNA, and linker histone form a unique structural motif that directs the higher-order folding and compaction of chromatin. Proc. Natl. Acad. Sci. USA. 95:14173-14178.

[7] Widom, J. 1986. J. Mol. Biol. 190:411-424.

[8] Chakravarthy S, Park YJ, Chodaparambil J, Edayathumangalam RS, Luger K, "Structure and dynamic properties of nucleosome core particles", FEBS Letters. (2005) Feb 7; 579 (4): 895-898

[9] K. V. Holde and J. Zlatanova, J. Biol. Chem. 270, 8373.

[10] K. V. Holde and J. Zlatanova, Proc. Natl. Acad. Sci. USA 93, 10548.

[11] Schalch T, Duda S, Sargent DF, Richmond TJ, "X-ray structure of a tetranucleosome and its implications for the chromatin fibre", Nature. (2005) Jul 7; 436: 138-141.

[12] C. L. Woodcock, S. A. Grigoryev, R. A. Horowitz, and N. Whitaker, Proc. Natl. Acad. Sci. USA 90:9021-9025.

[13] H. Schiessel, W. M. Gelbart and Robijn Bruinsma, Biophys J, April 2001, p. 1940-1956, Vol. 80, No. 4.

[14] Dorigo et al. Science 306, 1571.

[15] J. T. Finch and A. Klug, Proc. Natl. Acad. Sci. USA 73:1897-1901.

[16] J. Widom and A. Klug, Annu. Rev. Biophys. Chem. 43, 207.

[17] Kensal van Holde (1)(), Jordanka Zlatanova (1) (2) Chromatin Higher Order Structure: Chasing a Mirage? jbc ONLINE Volume 270, Number 15, Issue of April 14, pp. 8373-8376, 1995

[18] J. Bednar, R. A. Horowitz, J. Dubochet, and C. L. Woodcock, J. Cell. Biol. 131, 1365.

[19] J. Zlatanova, S. H. Leuba and K. van Holde, Biophys. J. 74, 2554.

[20] Leuba et. al. 1994. Proc. Natl. Acad. Sci. USA 91:11621-11625.

[21] S. E. Gerchman and V. Ramakrishhnan, Proc. Natl. Acad. Sci. USA 84, 7802.

[22] B. Mergell, R. Everaers and H. Schiessel Phys. Rev. E, 70, 011915-1-9.

[23] Barbi et al. Phys. Rev. E 71, 031910.

[24] H. Schiessel, 2003 J. Phys.: Condens. Matter 15, R699-R774.

[25] Diesinger, P. M., Heermann, D. W. 2006. Two-angle model and phase diagram for chromatin. Phys. Rev. E 74, 031904 (2006).

[26] Binder, K. and Heermann, D.W. 2002. The Monte Carlo Method in Statistical Physics, 4th Edition. Springer Series in Solid-State Sciences.

[27] Wolffe, A. 1999. Chromatin: Structure & Function, Academic Press Inc.,U.S. Third Edition.

[28] de Gennes, P.G. 1979. Scaling concepts in polymer physics. Cornell University Press, Ithaca 1979

[29] Bystricky, K., Heun, P., Gehlen, L., Langowski, J., Gasser, S. M. 2004. Long-range compaction and flexibility of interphase chromatin in budding yeast analyzed by high-resolution imaging techniques. Proc. Natl. Acad. Sci. U S A. 2004 November 23; 101(47): 1649516500.

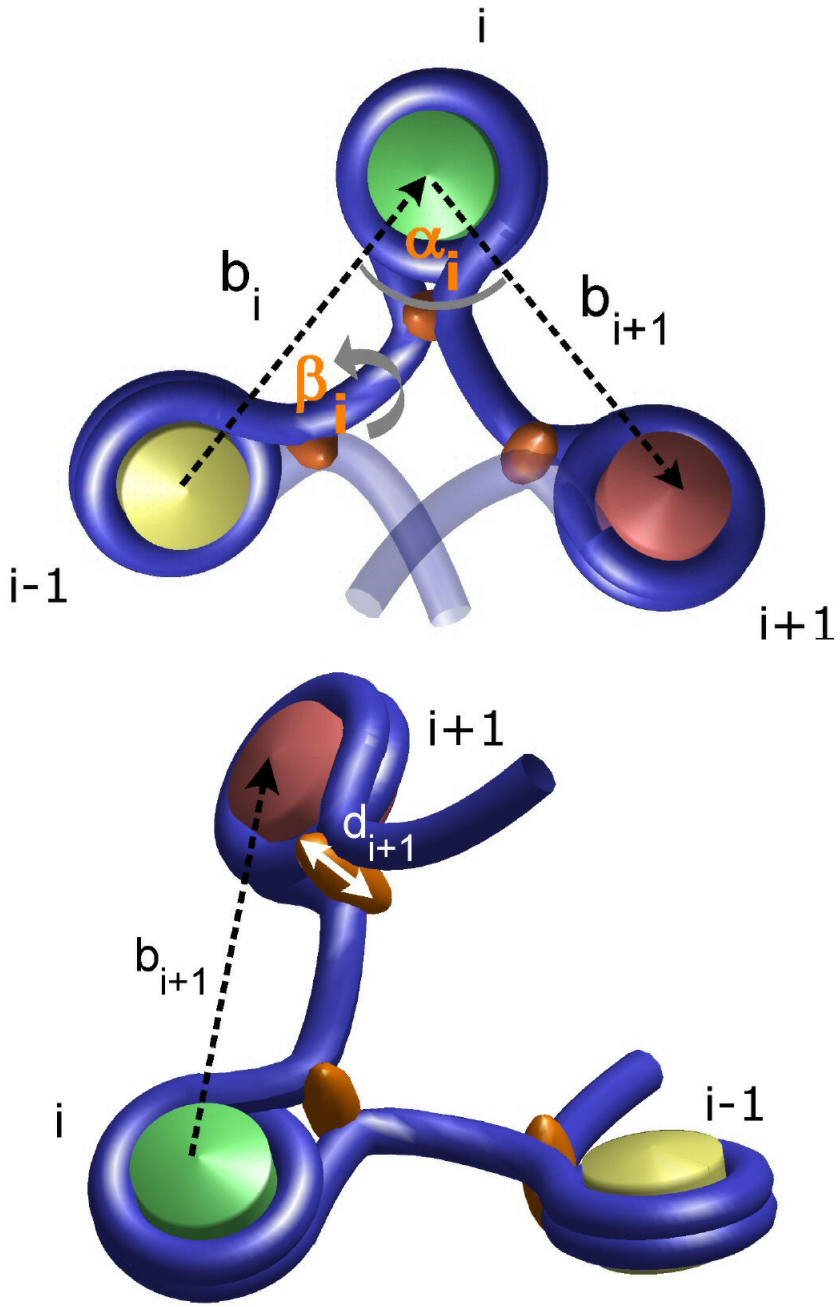

Figure 1: The figure shows the basic parameters of the E2A model: The entry-exit-angle α_i, the rotational angle β_i, the linker length b_i and the vertical distance d_i between in and outgoing linker. We chose a large entry-exit-angle here to make the visualization clear.

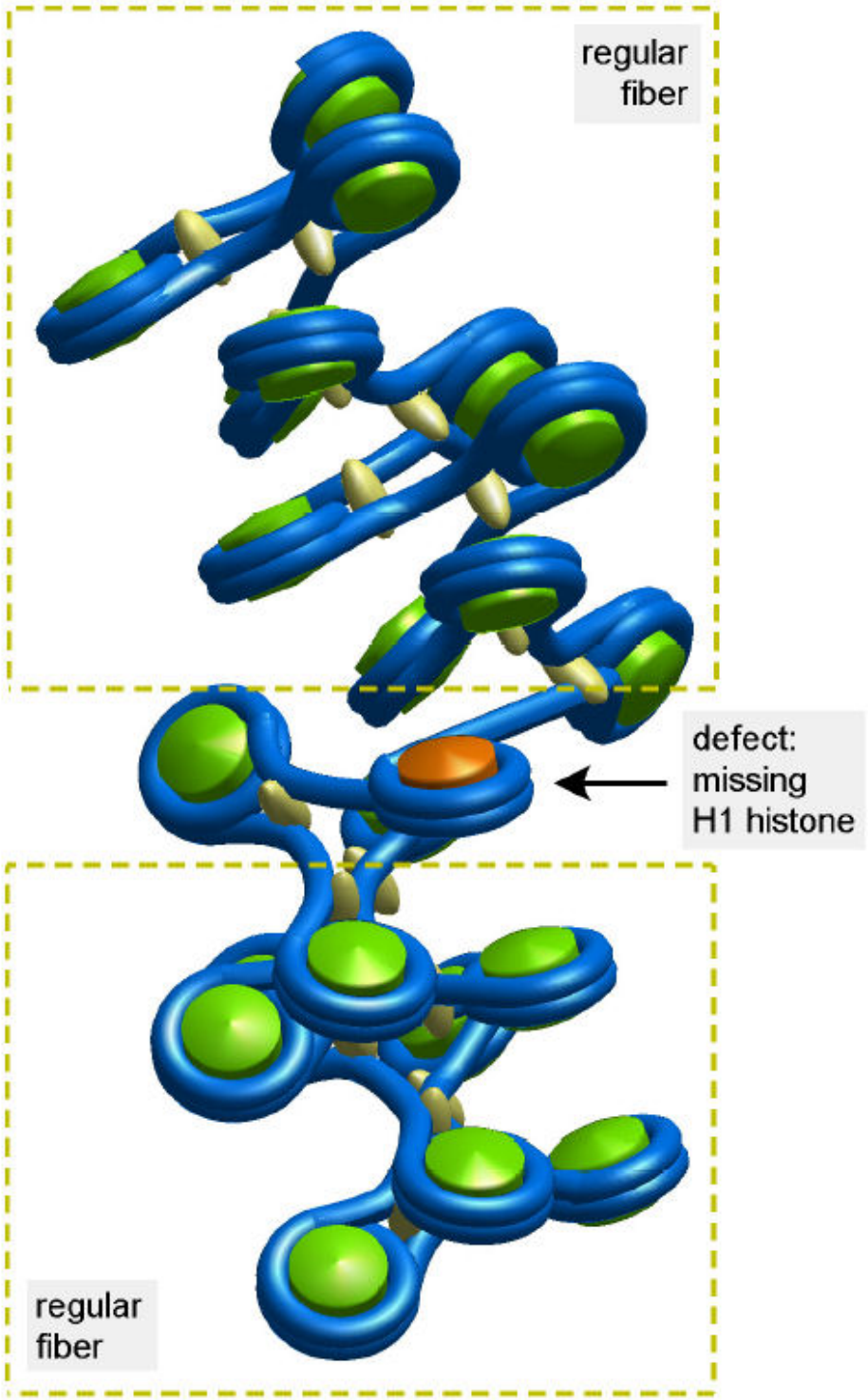

Figure 2: Shown is an example of a H1 defect within the chromatin fiber. The upper strand and the strand below the defect are regular.

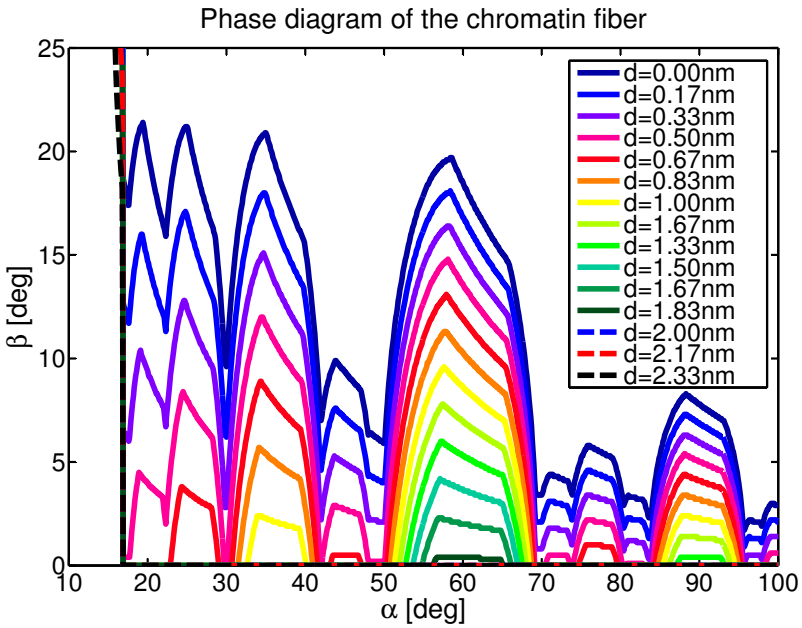

Figure 3: Cut-out of the chromatin phase diagram (for different d). The states below the corresponding lines are forbidden due to excluded volume interactions. With increasing d more and more states become accessible to the fiber.

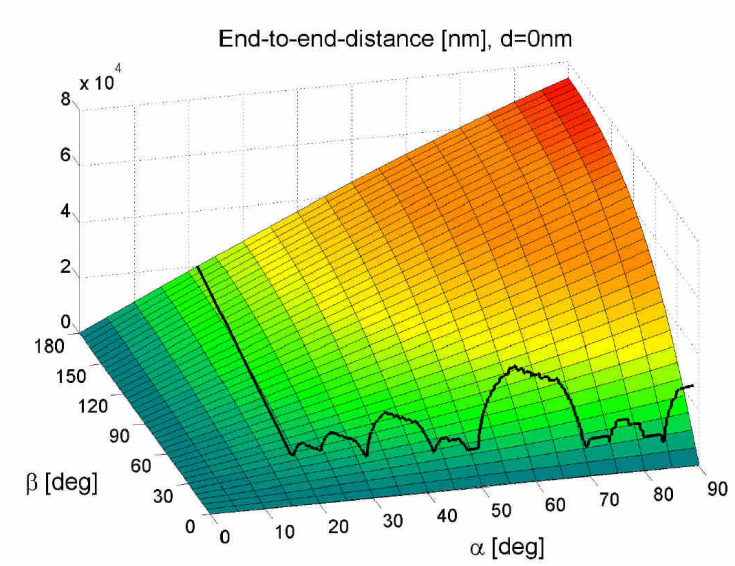

Figure 4: The end-to-end distance of regular chromatin fibers along a cut-out of the phase diagram with fixed fiber length (N=500 segments) and fixed d=0.0⟨bp⟩. The solid black line represents the corresponding phase transition.

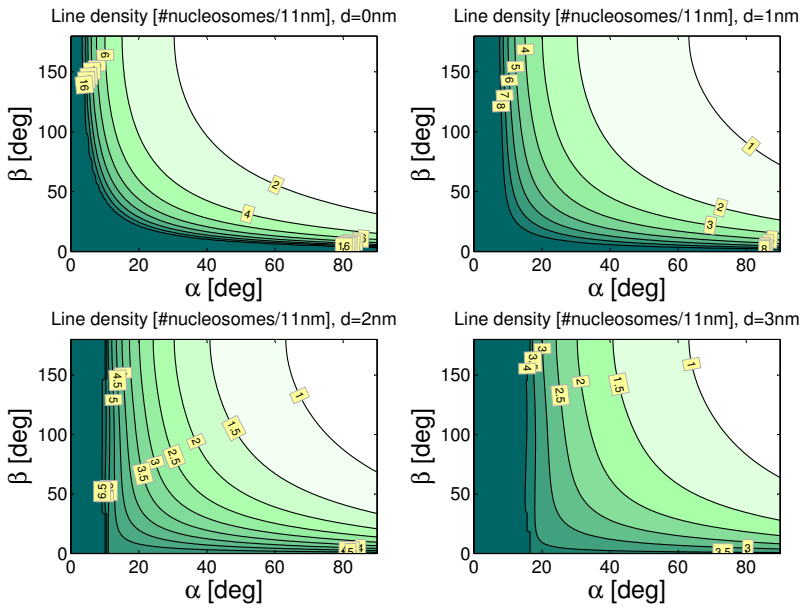

Figure 5: The line density of the nucleosomes within a regular chromatin fiber is large for small β_i. However the comparison with the phase diagram shows, that some of these states are forbidden due to excluded volume interactions.

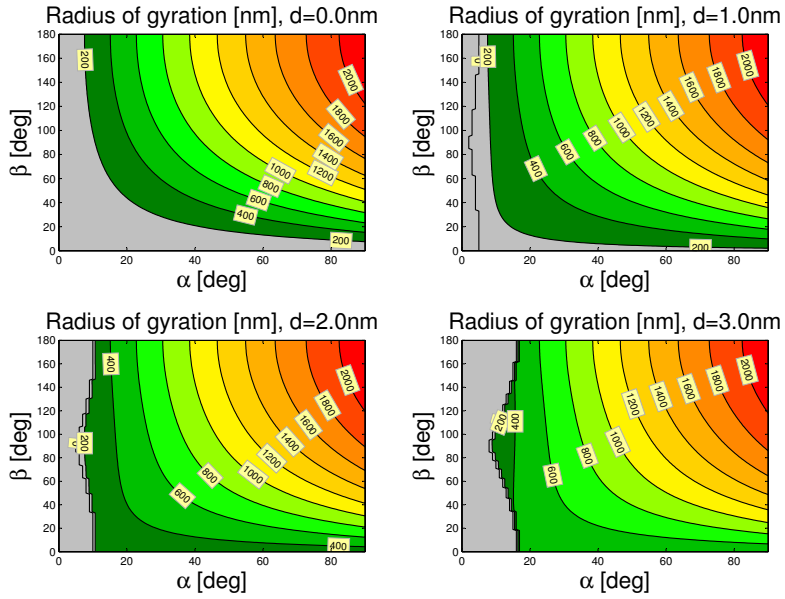

Figure 6: The radius of gyration of regular chromatin fibers along a cut-out of the phase diagram with fixed fiber length of N=500 segments. The compaction of the fibers decreases strongly with increasing d.

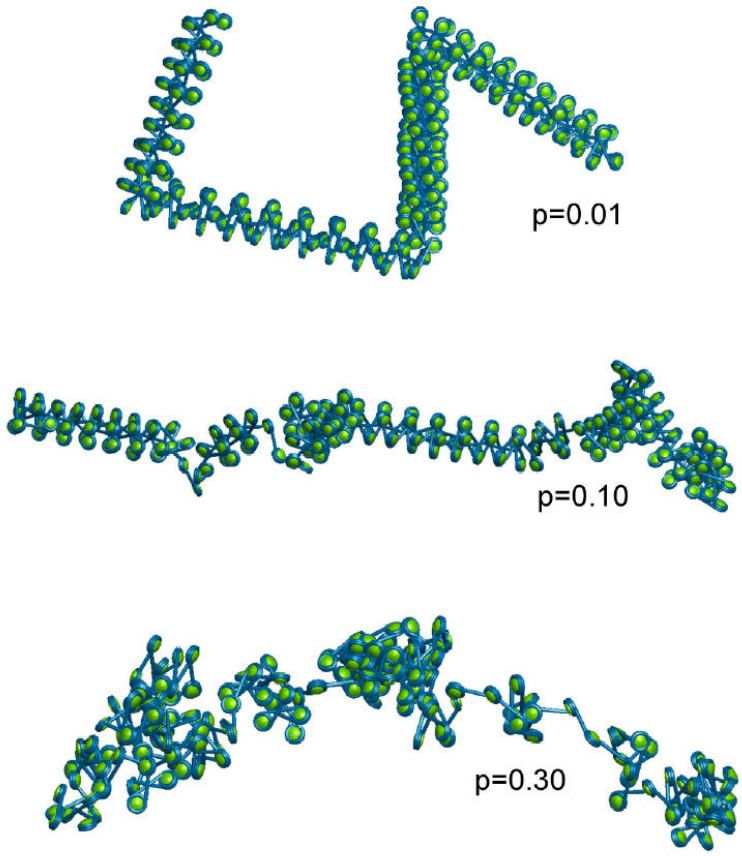

Figure 7: Chromatin fibers with different defect probabilities p. At $p = 0.30$ the regular structure of the 30nm strand is almost completely collapsed.

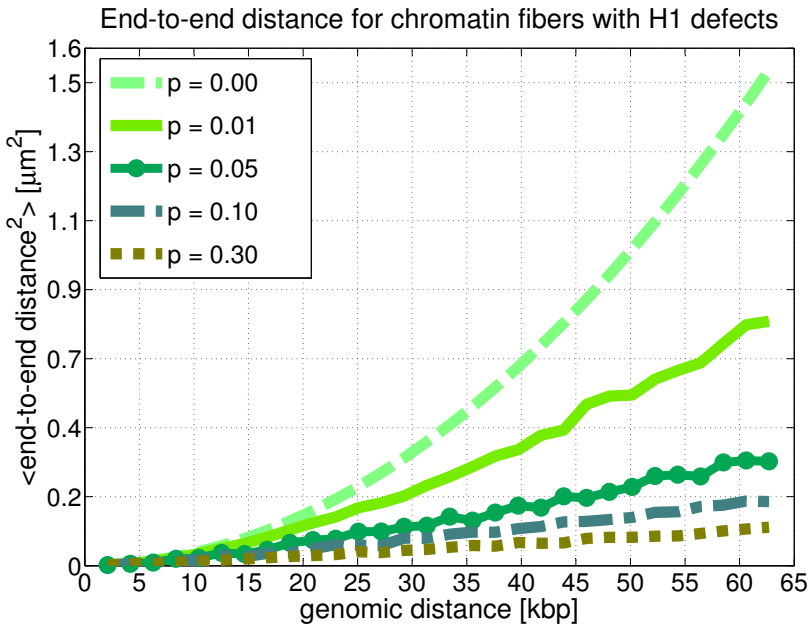

Figure 8: The mean end-to-end distance for chromatin fibers with H1 defects. With increasing defect probability p the length of the fibers decreases rapidly. H1 defects might play a crucial role for chromatin compaction.

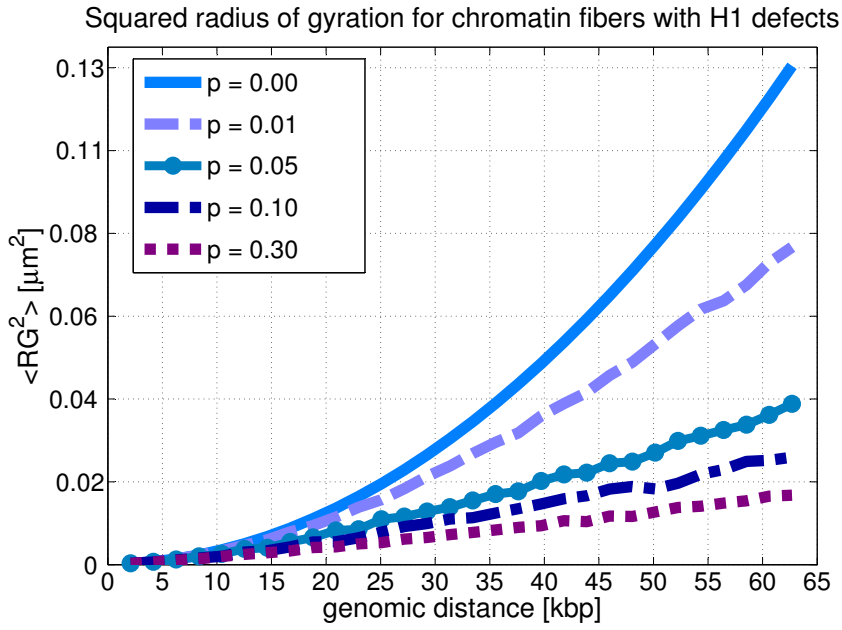

Figure 9: The squared radius of gyration for chromatin fibers with different defect probabilities p. With increasing number of H1 defects the fiber becomes much more compact which could be an important mechanism to compact the chromatin fiber.